Fuel 371 (2024) 132161

Contents lists available at ScienceDirect

Fuel

journal homepage: www.elsevier.com/locate/fuel

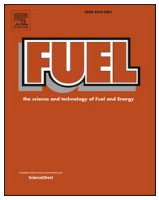

Full Length Article

Experimental investigation on diesel engine performance, combustion, and emissions characteristics with Tucuma and Ungurahui biodiesel blends

Arun Teja Doppalapudi [a,*], Abul Kalam Azad [a,*], M.M.K. Khan [b]

[a] School of Engineering and Technology, Central Queensland University, 120 Spencer Street, Melbourne, VIC 3000, Australia
[b] School of Engineering, Computer & Mathematical Sciences, Auckland University of Technology, Auckland, New Zealand

ARTICLE INFO

Keywords:
Fuel Modification
Combustion analysis
Emission formation
Prospective feedstock
Heat release rate
Biodiesel blends
NO_x emission

ABSTRACT

The study conducted an experimental investigation of diesel engine performance, emissions, and combustion characteristics using Tucuma and Ungurahui biodiesel blends. Higher yield (greater than 99.4%), lower viscosity than diesel, and higher cetane number of these fuels have motivated a comprehensive investigation of the effect of these fuels on diesel engines. Four blends were tested in the engine by keeping diesel as the benchmarking fuel. The engine was operated at full load conditions, and the results were investigated with respect to brake power (BP). Results indicate that biodiesel blends showed similar combustion behaviour to that of diesel. Next to diesel, TB10 and UB10 showed better brake thermal efficiency (BTE) and lower brake-specific fuel consumption (BSFC). Higher peak pressures and heat release rates (HRR) are observed for the TB10 compared to the diesel operation. Moreover, prolonged combustion was observed for the four biodiesel blends during the diffusion and late combustion phasing. With the increase in BP, slightly higher HC emissions are observed for all the blends except for TB10 compared to diesel. Similarly, a slight increase in CO emissions is also observed for all the blends at higher BP. Higher acid values of both fuels are the likely cause of increased HC and CO emissions at higher BP. NO_x emissions are slightly higher for both fuels, among these UB10 has shown lower NO_x than other blends. The study concludes that TB10 has demonstrated better performance (near diesel) and combustion rates (better than diesel); however, emissions like CO and NO_x are slightly higher than others. The study recommends blending TB10 and UB10 with the alcohols, ethers, and nanoparticles as they can reduce NO_x and CO emissions.

1. Introduction

In the transportation sector, diesel engines are significant consumers of fossil fuels and emit harmful greenhouse gas emissions [1]. At the same time, demand for diesel engines is also high because of their long-term durability and versatile applications in marines, agriculture, industries, and the mining sector [2]. The regulations to reduce the carbon footprint have significantly impacted the transportation energy structure. The rise in energy demands and prices and the depletion of fossil sources have opened the search for new clean energy sources with stringent regulations and goals to achieve sustainability in the transportation sector [3]. Recent studies have indicated that biodiesel is one of the alternative fuel sources for fossil fuel as it is a renewable type and has significantly reduced CO, HC, particulate matter, and sulfur emissions [4]. In 2020, the United States of America (USA) became the leading biodiesel producer, producing 200,000 barrels daily, 48 % of the world's total biodiesel production [5]. Followed by Brazil, accounting for 28 %, and Germany and China, accounting for 3 % of the entire world's biodiesel production, respectively [6]. According to the International Energy Agency (IEA) forecasts, the current production rate (main case), the biodiesel demand will increase by 52.9 billion litres in the next five years [7]. In the accelerated case, the demand will increase by 68.1 billion litres by 2028 [7]. Indonesia, the largest biodiesel producer in 2022, used mainly palm oil as the feedstock for biodiesel

Abbreviations: ASTM, American Standard Testing Method; BSFC, Brake Specific Fuel Consumption; BMEP, Brake Mean Effective Pressure; BP, Brake Power; BSEC, Brake Specific Energy Consumption; BTE, Brake Thermal Efficiency; CO, Carbon Monoxide; CO_2, Carbon Dioxide; EGT, Exhaust Gas Temperature; HC, Hydrocarbons; HRR, Heat Release Rate; ID, Ignition Delay; KOH, Potassium Hydroxide; MFB, Mass Fraction Burnt; NO_x, Nitrogen Oxide; OME, Oleic Methyl Ester; PME, Palmitic Methyl Ester; SOC, Start of Combustion; TB10, 10% Tucuma + 90% diesel by volume; TB20, 20% Tucuma + 80% diesel by volume; UB10, 10% Ungurahui + 90% diesel by volume; UB20, 20% Ungurahui + 80% diesel by volume.

* Corresponding authors at: School of Engineering and Technology, Central Queensland University, 120 Spencer Street, Melbourne, VIC 3000, Australia.
E-mail addresses: a.doppalapudi@cqu.edu.au (A.T. Doppalapudi), a.k.azad@cqu.edu.au, azad.cqu@gmail.com (A.K. Azad).

https://doi.org/10.1016/j.fuel.2024.132161
Received 5 February 2024; Received in revised form 9 May 2024; Accepted 5 June 2024
Available online 8 June 2024

production [8]. Meanwhile, the USA primarily uses soybean oils as feedstock for biodiesel production. Still, other major countries depend on edible feedstocks and seed oils to produce biodiesel [9]. Extensive investigations have been conducted worldwide for the non-edible feedstock termed the second-generation feedstock for biodiesel production [10].

A variety of feedstocks were used to prepare biodiesel fuels to make their production more economically viable. Second-generation feedstocks are one of the most viable sources for producing biodiesel as they have high lipid content and are widely available. Non-edible, eco-friendly, low production cost and the fact that it can be cultivated in barren lands are the advantages of the second generation of biodiesel fuels [11]. A few second-generation biodiesel feedstocks such as Jatropha, Karanja, Calophyllum Inophyllum [12], Neem [13], Mahua [14] and Rubber seed [15] oils are widely investigated and reported. It is found that fatty acid methyl esters influence the combustion and emissions parameters. The fatty acid profiles affect biodiesel properties such as oxidative stability, cloud point, density, kinematic viscosity and cetane number [16]. Major fatty acid compositions are Methyl palmitate ($C_{17}H_{34}O_2$, C16:0), Methyl oleate ($C_{19}H_{36}O_2$, C18:1), Methyl stearate ($C_{19}H_{38}O_2$, C18:0) and Methyl linoleate ($C_{19}H_{34}O_2$, C18:2). For instance, oleic methyl ester (OME) has the higher molecular weight 296.5 g/mol [17], compared to palmitic methyl ester (PME) 270.45 g/mol [18], hence high density is noted for biodiesel with high OME content than PME. For instance, there is more OME content in Jatropha (60.70 wt%) than soybean (23.70 wt%), and higher density is noted for the Jatropha than soybean [19]. The composition of fatty acid methyl esters governs the biodiesel fuel properties [20]. The physiochemical property of the biodiesel varies with the feedstock type, and plenty of other feedstock needs attention. Hence, the study reviewed over 150 feedstocks and their fatty acid profiles and selected Tucuma and Ungurahui as new feedstocks because of their high lipid fat content. Their usage in diesel engines was tested and presented in this study [21–25].

A comprehensive investigation is needed for the Tucuma and Ungurahui to study their effect on diesel engine performance and emissions. Tucuma and Ungurahui fatty acid contents are similar to other biodiesel feedstocks such as Rapeseed [26], soybean [27], Jatropha [28], palm [28], P. chinesis [29], waste cooking oil [30] and others. However, the combustion behaviours will differ for all the biodiesel types as their FAME composition varies individually. For instance, Shameer and Ramesh [31] conducted engine tests with waste cooking oil and camphor oil and found that the fuel combustion rates varied from feedstock to feedstock. Lower brake thermal efficiency (BTE) and lower peak cylinder temperatures are noted for camphor biodiesel with reduced NO_x emissions. Several researchers revealed that biodiesel engine tests showed increased brake thermal efficiency (BTE) [32,33], increased brake specific fuel consumption (BSFC), reduced carbon monoxide (CO) and hydrocarbon (HC) [34], and increased Nitrogen oxides (NO_x) emissions [35]. Biodiesel fuels have exhibited several interesting factors due to their physical composition, operating conditions, and their blend mixing proportions. For instance, Habibullah et al. [36] conducted experimental analysis with coconut and palm oil biodiesel blended with diesel. The study reported a reduction in CO and HC by 13.75 % and 17.97 %, respectively, for both fuels compared to diesel fuel operation. However, palm oil has higher NO_x than coconut biodiesel [36]. The main reason behind reduced NO_x for coconut oil is the presence of higher saturated fatty acids [37].

The scope of this article is to present the effect of two new feedstocks, Tucuma and Ungurahui, and their behaviours during engine operation. During the biodiesel conversion process, both oils showed higher conversion yields greater than 99.4 %, and this has drawn much attention and motivated authors to further investigate the effect of these oils on diesel engines. Hence, the study further aims to examine how Tucuma and Ungurahui biodiesel blends affect diesel engine performance, combustion, and emissions. The experiments were conducted at full load conditions with speeds ranging from 1200 rpm to 2400 rpm. The test results are presented showing the effect of performance and emission patterns with respect to the power (BP).

The biodiesel conversion process, blending of Tucuma and Ungurahui oils, and the physiochemical properties and FAME composition of these fuels are presented in the article. Biodiesel engine performance parameters such as BTE, BSFC, volumetric efficiency, brake mean effective pressure (BMEP) and BSFC are reported with respect to BP. The emission parameters, including CO, carbon dioxide (CO_2), HC and NO_x are presented. Combustion parameters are investigated with respect to fuel heat release rates (HRR), in-cylinder pressures and mass fraction burnt (MFB). Finally, the study presents its major findings and recommendations from this investigation.

2. Materials and methods

2.1. Materials

Tucuma and Ungurahui oils were obtained from the renowned USA-based company – Nature in Bottle. Tucuma and Ungurahui are native to the Amazon, and their pulp contains high lipid content [38]. Tucuma has 40 to 75 % lipids in its pulp and approximately 40 % in its kernels [39]. Hence, these high-lipid, non-edible oils can serve as the prospective feedstock for biodiesel production [40]. Similarly, Ungurahui oil is also a family of *Arecaceae* (palm) that needs to be adulterated before being used as an edible oil. Ungurahui is also rich in lipid content and has 51.6 % of the dry weight of oil [41], which is higher than the sunflower (up to 45 %), Canola (40 % to 45 %) and Olive (18 % to 35 %) [42,43]. Westlab Pty. Ltd. Australia supplied high-grade potassium hydroxide (KOH) and methanol for transesterification. Finally, the diesel fuel is obtained from the Ampol Petroleum Company and used for engine operations and biodiesel blends.

2.2. Biodiesel conversion and its blend preparation

Tucuma and Ungurahui biodiesel fuels were produced from the transesterification process utilizing optimized parameter conditions. The transesterification process converts triacyl-glycerides in the bio-oil to methyl esters, yielding glycerol as a byproduct. Tucuma and Ungurahui oils are mixed with methanol in the presence of active catalyst potassium hydroxide (KOH) at optimized temperature and time conditions. A total of 27 experiments were conducted at three levels: catalyst range (0.5 wt% to 1.5 wt%), Methanol to oil molar ratio (5:1 to 7:1), reaction temperature (50 °CA to 70 °CA) and reaction time (50 min to 70 min). The optimized conditions for producing Tucuma and Ungurahui biodiesel fuels were achieved using the response surface method in conjunction with a Box-Behnken design matrix. For Tucuma biodiesel, a 7:1 methanol to oil molar ratio, 0.5 % (w/w) KOH catalyst amount, 70 min reaction time, and 53 °CA temperature conditions are used to yield 99.6 %. Whereas for Ungurahui biodiesel, a 5.9:1 methanol to oil molar ratio, 0.5 % (w/w) KOH catalyst amount, 50 min reaction time, and 70 °CA temperature conditions were used to yield 99.5 %.

The biodiesel blends were prepared by keeping fossil diesel as the baseline fuel. Biodiesel blends were modified with different proportions of biodiesel content while maintaining the baseline diesel in the mixture. That means TB10 (10 % Tucuma + 90 % diesel by volume), TB20 (20 % Tucuma + 80 % diesel by volume), UB10 (10 % Ungurahui + 90 % diesel by volume) and UB20 (20 % Ungurahui + 80 % diesel by volume). The biodiesel and diesel blends are prepared as a batch of 4 L in a five liters conical flask using a magnetic stirrer. The stirrer was maintained at a constant speed of 500 rpm at temperatures around 26 ± 1.5 °CA for a duration of 60 min.

2.3. Fuel characterization and FAME test

Table 1 presents the percentages of fatty acid methyl esters (FAME)

Table 1
FAME composition of Tucuma and Ungurahui biodiesel fuels.

Methyl ester name	Profile	Tucuma (% area)	Ungurahui (% area)
Dodecanoic	C12:1	0.33	–
Tetradecanoic	C14:1	1.72	0.56
Palmitic	C16:0	25.69	23.80
Palmitoleic	C16:1	0.162	0.12
Heptadecanoic	C17:0	0.182	–
Stearic	C18:0	11.79	96.
Oleic	C18:1	44.87	52.11
linoleic	C18:2	12.56	10.64
Linolenic (6, 9, 12)	C18:3	0.1	–
Linolenic (9, 12, 15)	C18:4	0.16	0.15
Eicosanoic	C20:1	0.87	0.72
11-Eicosenoic acid	C20:2	0.17	0.21
Docosanoic acid	C22:0	1.02	1.71
Tetracosanoic acid	C24:0	0.35	0.37
Total peak area		100	100
Total unsaturated %		58.04	63.23
Total saturated %		41.97	36.77

in Tucuma and Ungurahui biodiesel fuels. FAME tests were conducted using Gas chromatography- Mass spectrometry, where the individual tests were carried out for each sample, and the averages of each sample were presented in Table 1. Tucuma methyl esters contain mainly oleic (448.87 %), palmitic (25.69 %), linoleic (12.56 %) and stearic (11.8 %). Ungurahui has mainly oleic (52.11 %), palmitic (23.80 %), Linoleic (10.64 %), and stearic (9.56 %). The composition range for both Tucuma and Ungurahui is similar because they belong to the same family of *Arecaceae*. The physicochemical properties of biodiesel were measured in accordance with the corresponding ASTM biodiesel standards to ensure the fuel's suitability for engine tests and are presented in Table 2. The density for each sample was tested using ASTM D1298 standards at 15 °CA, where the density of Ungurahui (880.3 kg/m^3) exceeds that of Tucuma (879.1 kg/m^3) methyl ester. The higher density is primarily attributed to the higher content of methyl oleate in Ungurahui than in Tucuma. Viscosity for both fuels is noted at 4.0 mm^2/s at 40 ℃, which closely resembles that of diesel fuel. The calorific value of Tucuma (39.87 MJ/kg) is observed to be higher than Ungurahui (39.82 MJ/kg), but both fall short in comparison to diesel (45.7 MJ/kg). Table 2 shows higher flash, cloud, and pour points observed for Tucuma and Ungurahui than diesel. This is due to vegetable oils have higher flash and fire points [44]. These properties affect the cold flow properties, mainly due to saturated fatty acids. These saturated fatty acids have higher melting points than unsaturated fatty acids [45]. Unsaturated fatty esters are less in Tucuma (58.03 %) than in Ungurahui (63.23 %). Meanwhile, saturated fatty acids are more prevalent in Tucuma (41.9 %) than in Ungurahui (36.7 %). The cloud point mainly depends on saturated fatty acids and is higher for Tucuma (8 ℃) than Ungurahui (6 ℃). Higher acid values are noted for Ungurahui than in Tucuma. Moreover, the Ungurahui acid value is slightly higher than the standard biodiesel. Overall, as per ASTM D6751 standards, favorable properties are noticed in both the biodiesel blends and indicating their suitability for use in diesel engines.

Table 2
Physicochemical properties of Tucuma and Ungurahui biodiesel fuels as per ASTM standards.

Property	Test standard	Tucuma	Ungurahui	ASTM D6751 standard biodiesel [46]	Diesel
Density at 15 °C (kg/m^3)	ASTM D1298	879.1	880.3	860–890	832
Viscosity at 40 °C (mm^2/s)	ASTM D445	4.0	4.0	1.9–6.0 mm^2/s	4.1
Calorific value (MJ/kg)	ASTM D240	39.87	39.82	–	45.7
Cetane index	ASTM D613	48.2	48.2	Min^m 47	44
Flash point	ASTM D93/IP 34	186	176.5	Min^m 100	62
Cloud point (°C)	ASTM D2500	8	4	Report	−8.6
Pour point (°C)	ASTM D97/IP 15	6	−6	–	−15
Acid value (mgKOH/g)	ASTM D664	0.47	0.56	Max^m 0.5	–

2.4. Engine setup and experimentation

Fig. 1 presents the schematic diagram illustrating the experimental setup of the Kubota V3300 4-stroke diesel engine test rig that was employed to perform tests. The setup consists of an engine, an eddy current dynamometer, a data acquisition system, and a 5-gas analyzer. The engine specifications are summarized in Table 3 [47,48]. The experiments were conducted under full load conditions and varied speeds to examine the performance, combustion, and emission characteristics according to the SAE J1995 engine test standard. Before taking the reading, the throttle was set to a maximum, and the engine was operated at 1200 rpm for 10 min to ensure its stability. The initial tests were conducted using pure diesel fuel, and the readings were recorded using data acquisition systems. Subsequently, a similar procedure was continued with the biodiesel blends. At each run, the leftover fuel was pumped from the tank to let the target fuel pass into the engine cylinder. Moreover, the engine was allowed to run for 10 min before recording the new data set with new fuel blends. During all the experiments (diesel, TB10, TB20, UB10, and UB20), the engine was maintained at full load condition, while the speed was adjusted within the range of 1200 rpm to 2400 rpm, with a stepwise increment of 200 rpm. Two sets of data were recorded for each experiment at different time intervals to ensure the precision of the recorded data.

2.5. Theoretical evaluation

2.5.1. Performance parameters estimation

1) Brake power (BP) represents the power obtained at the engine shaft output, and the engine BP can be calculated using Eq. (1) [49].

$$BP = \frac{2\pi NT}{60 \times 1000} \tag{1}$$

where BP is in kW, T refers to the engine's torque in N.m, measured using a dynamometer, and N denotes engine speed in rpm.

2) Brake thermal efficiency is the amount of work produced from the fuel energy supplied and estimated from Eq. (2) [50].

$$BTE(\%) = \frac{BP}{m_f \times Fuelcalorificvale} \tag{2}$$

where m_f is the mass flow rate of the fuel in kg/hr.

3) Brake-specific fuel consumption (BSFC) refers to the rate of fuel consumption rate with respect to the engine power and can be computed using Eq. (3) [49].

$$BSFC(kg/kW.h) = \frac{m_f}{BP} \tag{3}$$

4) Brake mean effective pressure is estimated from Eq. (4).

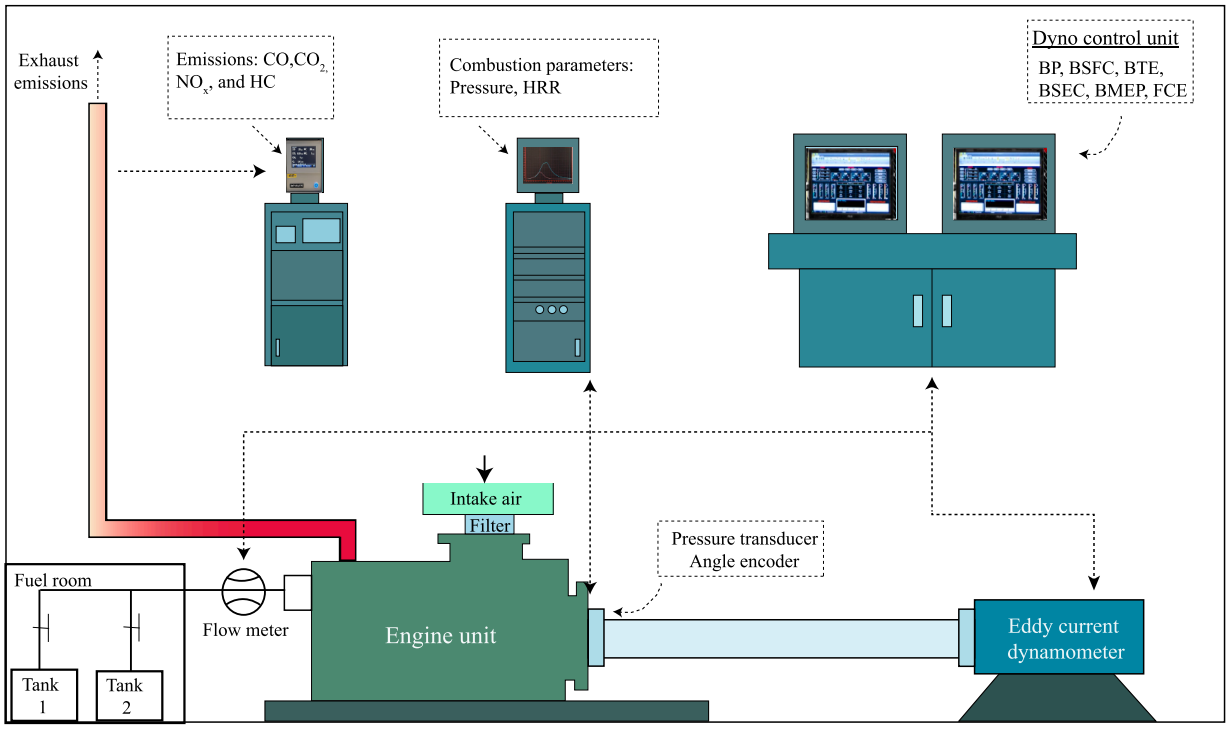

Fig. 1. Schematic diagram of engine test equipment.

Table 3
Specification of the engine and emission analyzer.

Engine Specification		Accuracy of emission analyzers	
Engine model	Kubota V3300	Parameter (range)	Accuracy
Type	Vertically water-cooled	O_2 (0–25 %vol)	±0.1 % abs
Number of cylinders	4	NO_x (0–5000 vol ppm)	±20 ppm abs
Bore x stroke (mm)	98 x 110	HC (0–3000 ppm vol)	±4 ppm abs
Total displacement	0.003318 m^3	CO (0–15 %vol)	±0.02 % abs
Compression ratio	22.6:1	CO_2 (0–20 %vol)	±0.3 % abs
Injection timing	16 °CA before TDC		
Injection pressure	13.73 Mpa		

$$BMEP(bar) = \frac{BP \times 60}{L \times V \times \left(\frac{N}{n}\right) \times No.ofcylinders \times 100} \tag{4}$$

L represents stroke length (m), A refers to piston volume (m^3), and n is 2 for four-stroke engines.

5) Volumetric efficiency is the ratio of air intake to the engine swept volume and can be calculated using Eq. (5).

$$\eta_v(\%) = \frac{BP \times 60}{L \times A \times \left(\frac{N}{n}\right) \times No.ofcylinders \times D_{air} \times 60} \times 100 \tag{5}$$

where D_{air} is the density of air in Kg/m^3

6) Brake specific energy consumption (BSEC) is to evaluate the engine performance and can be calculated using Eq. (6) [51].

$$BTE(\%) = \frac{m_f \times Fuelcalorificvale}{BP} \tag{6}$$

2.5.2. Combustion parameter estimation

1) Heat release rate (HRR) was derived from the pressure values using the first law of thermodynamics, which can be calculated using Eq. (7) [52].

$$\frac{dQnet}{d\theta} = \frac{\gamma}{\gamma - 1} p \frac{dV}{d\theta} + \frac{1}{\gamma - 1} v \frac{dP}{d\theta} \tag{7}$$

where Q_{net} is the heat release rate (J/°CA), v and p denote in-cylinder volume (m^3) and pressures (Pa) at that crank angle, and γ indicates the ratio of specific heats.

2) The mass fraction burnt inside the cylinder helps identify the start and finish of the combustion and can be calculated using Eq. (8), [53,54].

$$MFB = \frac{\sum_0^i \Delta_P}{\sum_0^N \Delta_P} \tag{8}$$

where Δ_P is the pressure rise during the change of each crank angle.

3. Results and discussions

3.1. Performance graphs

3.1.1. Variation of BTE and BSFC with respect to BP

Fig. 2 illustrates the BTE and BSFC with respect to BP. BTE and BSFC are the primary indicators used to determine engine performance. BSFC indicates the energy consumption rate, whereas BTE provides information on the energy utilization rate. BSFC has shown an inverse trend to the BTE with respect to BP. Compared to other biodiesel fuels, diesel showed a notable decrease in BSFC. For all the fuels, the BTE trend increases with increasing BP and decreases with further increases in BP. The maximum BTE was observed for diesel (35.45 %), followed by TB10 (31.95 %) and TB20 (31.36 %) at mid-BP conditions. Meanwhile, for Ungurahui blends UB10 (31.91 %) and UB20 (31.31 %), higher BTE is observed after the mid-BP (mid-speed conditions). Diesel has the highest

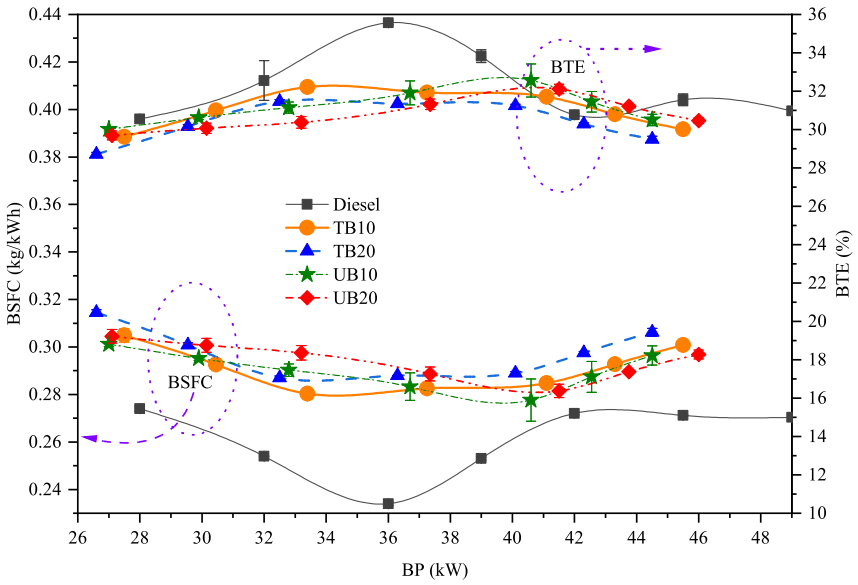

Fig. 2. Effect of variation in BP with respect to BTE and BSFC.

calorific value, followed by Tucuma and Ungurahui; hence, the BTE trend is in the range of higher to lower calorific value of the fuels. As seen in Fig. 2, for all the fuels, reduced BSFC is observed with increased BP (till mid-speed conditions), and an increase in BSFC trend is noted with a further increase in BP. At lower BP, BSFC for TB10, TB20, UB10 and UB20 fuels increased by 9.09 %, 14.8 %, 9.49 % and 10.72 %, respectively, compared to diesel. Similarly, at higher BP, BSFC is increased for TB10, TB20, UB10 and UB20 fuels by 10.53 %, 10.83 %, 9.21 % and 9.35 %, respectively, compared to diesel. At lower BP (lower speeds), higher BSFC results from increased time-lapse for heat losses from combusted gas to the cylinder chamber. The difference in the trend between diesel and biodiesel fuels is mainly due to the time available to complete one cycle. At lower speeds, BSFC rises due to prolonged time duration for heat losses from the gas to the cylinder and piston wall [55]. At high speeds, the time available for combustion causes a lapse for biodiesel (lower energy fuel) combustion than diesel fuel. Throughout the injection period, the higher bulk modulus of the biodiesel causes it to slip more into the combustion chamber, even when injected at the same rate as diesel [56,57]. The difference in physical properties of biodiesel, such as its higher density and viscosity, causes an inefficient distribution of fuel droplets, thereby causing inferior volatility to injected fuel particles. The combustion rates became poorer in such conditions as these rates highly depend on the mixture-based conditions [58]. Hence, to achieve the desired rated power output, higher amounts of biodiesel are required than diesel.

3.1.2. *Variation of volumetric efficiency and BMEP with respect to BP*

Fig. 3 shows the effect of BP on the engine's volumetric efficiency and BMEP. The engine's volumetric efficiency decreases with increasing BP (increasing speed) for all the fuel blends. This is mainly due to airflow restrictions in the air filter, intake manifold, and intake valves at high speeds [59]. These restrictions impact the volumetric losses of air entering the system. The adequate time for filling the engine cylinder with the charge at low speeds leads to higher volumetric efficiency. According to Ağbulut et al. [60], higher volumetric efficiency increases the combustion period and decreases the heat and friction losses and gas

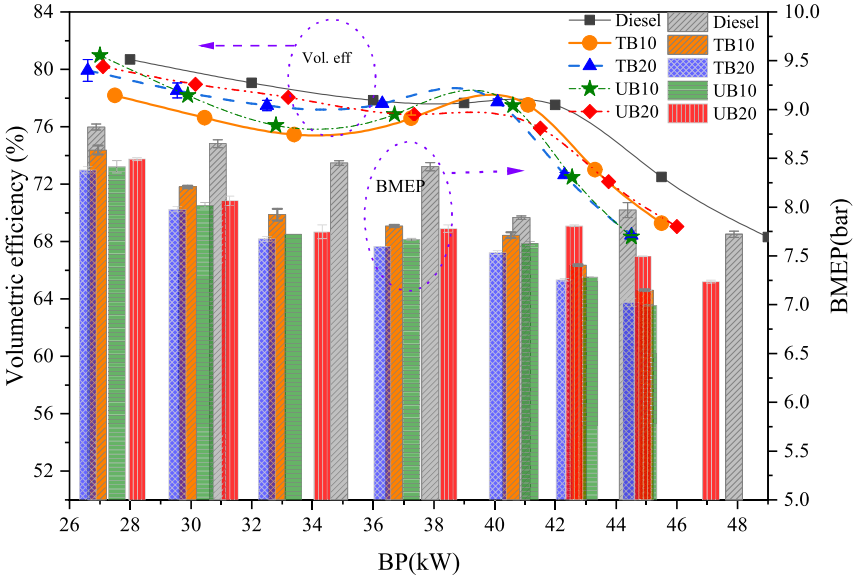

Fig. 3. Effect of variation in BP with respect to volumetric efficiency and BMEP.

leakages. At low BP, higher volumetric efficiency is noted for diesel (80.68 %), followed by UB10 (80.97 %), UB20 (80.18 %), TB20 (79.92 %) and TB10 (78.19 %). At higher BP, lower volumetric efficiency is noted for TB10 (68.26 %), followed by diesel (68.31 %), UB10 (68.32 %), TB20 (68.43 %) and UB20 (69.05 %). It is evident from Fig. 3 that biodiesel experiences a more pronounced reduction in volumetric efficiency compared to diesel fuel. This is because the elevated temperatures caused by the higher BSFC impact the mass of the drawn air. Also, higher temperatures (either due to high speeds or high loads) inside the chamber reduce the mass of intake air, consequently lowering the volumetric efficiency [59]. The volumetric efficiency is also involved with the BMEP as the BMEP, as it is the pressure imposed on the piston head. Both volumetric efficiency and BMEP showed a reduced trend with the increasing BP.

3.1.3. Variation of EGT and BSEC with respect to BP

Fig. 4 presents the comparison of EGT with the BSEC with respect to the BP. With the increasing BP, BSEC is reduced till mid-BP and increases with further increase in BP. The variations presented in Fig. 4 are calculated as the relative values at varying BP. The BSEC is higher for biodiesel fuels than diesel fuel; moreover, it is noted that BSEC increases with the increasing proportion of biodiesel in the blend [61]. As presented in Fig. 4, TB20 showed higher BSEC compared to TB10 at all BP conditions. Similar findings have been reported in studies conducted by Emma et al. [62] and Venu et al. [63]. EGT increases with the increasing BP, and biodiesel exhibited higher EGT compared to diesel because of the higher specific fuel consumption. Ungurahui oil has a higher EGT because both UB10 and UB20 have lower energy content, necessitating increased fuel consumption to compensate for the rated power [64]. The higher specific fuel consumption values increase the combustion temperatures and elevate the EGT [65]. Among the Tucuma blends, TB10 has shown higher EGT than TB20. At mid BP 34 kW to 42 kW, TB10 has shown lower EGT compared to UB10, and UB20, but at higher BP, TB10 has shown a slight increase in EGT compared to other blends.

3.2. Emissions

3.2.1. Impact of BP on HC emissions

Fig. 5 demonstrates the comparison of HC and EGT with respect to the brake power. In diesel engines, unburnt hydrocarbon emissions are formed mainly due to improper combustion [66]. Indeed, biodiesel has a significant effect on reducing HC emissions. However, these emissions also depend on engine design and injection rates [67]. For instance, heterogeneous mixture formation (lean/rich), fuel wall wetting to the cold cylinder walls [68], cylinder chamber crevice volume, irregular piston bowl and engine operating conditions [50,69]. Higher HC emissions are observed at lower BP and then decrease with the increasing BP. At low BP (lower speeds), a small amount of fuel is injected with large amounts of excess air into the chamber. The insufficient formation of air–fuel mixture inside the chamber causes the poor distribution of fuel, which reduces the mean gas temperature. The unburnt lean mixture that escapes through exhaust causes higher HC emissions at lower speeds. The effect of biodiesel on the HC emissions can be seen in Fig. 5. Diesel fuel has higher HC emissions, followed by UB10, TB10, UB20 and TB20. The trend suggests that the HC emissions decrease with the increase in biodiesel in the blend. Though better combustion happens for diesel fuel, higher HC emissions are noticed in the BP range of 28 kW to 36 kW. This is due to the chemical structures of biodiesel, where HC gets

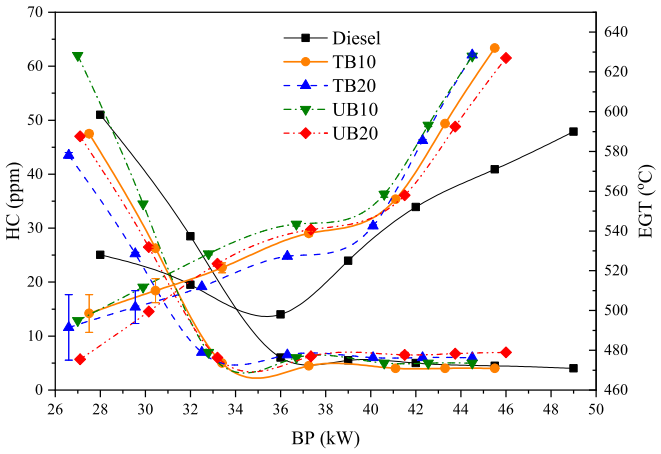

Fig. 5. Effect of Tucuma and Ungurahui oils on HC emissions with respect to BP.

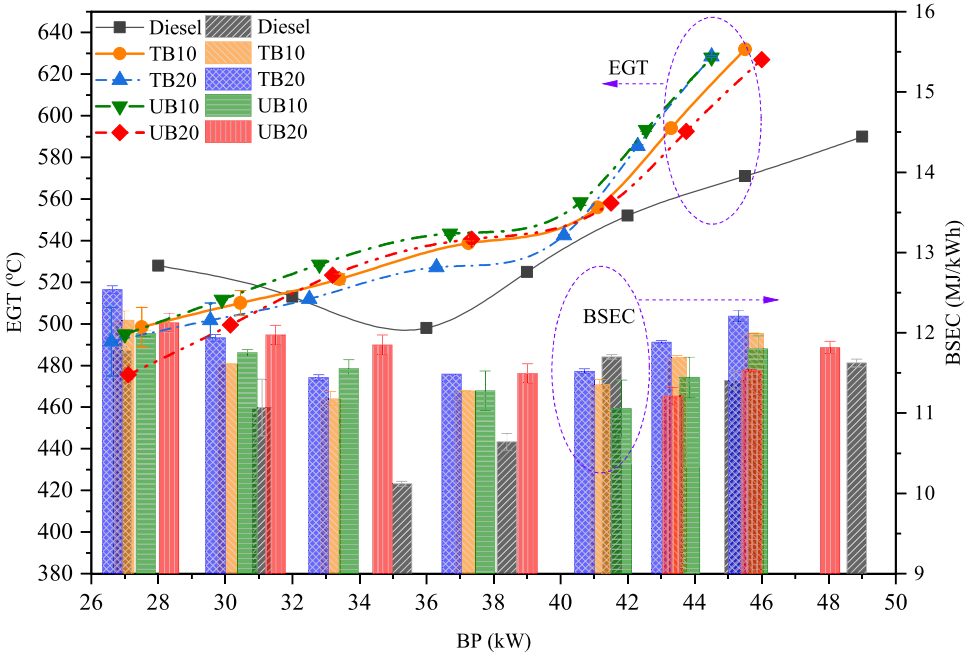

Fig. 4. Effect of variation in BP with respect to EGT and BSEC.

oxidized because of higher oxygen content in the biodiesel [70]. For instance, Liu et al. [38] observed a similar trend, where the team reported that four different biodiesel and ethanol blends revealed lesser HC emissions than pure diesel. It is also notable that HC emissions are higher at higher speeds for the TB20, UB10 and UB20 biodiesel blends. This is mainly because of the higher acid value of the Tucuma and Ungurahui biodiesel. Higher cetane numbers of Tucuma and Ungurahui biodiesel also affect the combustion delay, impacting the HC emissions [71]. A higher cetane number reduces the ignition delay, and at high speeds (higher BP ranges), less time is available for the HC emissions to get oxidized. At the same time, high-density biodiesel takes time to get adequately combusted in the span of microseconds. Hence, higher HC emissions are noticed for biodiesel than diesel at BP 36 kW to 49 kW. Overall, TB10 has shown better results than all the other blends, including benchmarking diesel fuel.

3.2.2. Effect of BP and EGT on NO_x emissions

For all the fuels, the NO_x emissions increased from 39 kW to 41 kW and then decreased. There are several arguments stating that the presence of higher oxygen content in biodiesel causes higher NO_x emissions [57]. Due to the lower calorific value of the biodiesel, more significant amounts of biodiesel premixed charge get combusted inside the chamber and cause higher NO_x emissions. Several authors argue that higher speeds generate high temperatures due to increased power generation, consequently leading to elevated NO_x emissions [72,73]. An increase in dynamic power increases the temperatures, which can impact NO_x levels. However, upon examining the NO_x trend in Fig. 6, it is evident that diesel exhibited higher BP compared to biodiesel fuels, yet NO_x emissions are lower for diesel fuel. It is mainly due to the higher BSFC, that has caused higher in-cylinder temperatures for the biodiesel. Though biodiesel has consumed more fuel, it has not compensated for BP as diesel has. Additionally, biodiesel combustion has shown elevated temperatures due to higher fuel consumption. As can be seen from Fig. 6, higher EGT is noticed for biodiesel fuels than diesel. The study has considered peak cylinder temperature conditions as a reference with EGT, as both are directly proportional. The EGT for UB20 is higher, hence the higher NO_x emissions. Though UB20 has revealed more elevated BP, it has high EGT, which has caused higher NO_x emissions.

3.2.3. Effect of BP on CO and CO_2 emissions

Fig. 7 illustrates the CO and CO_2 emissions with respect to BP for both Tucuma and Ungurahui biodiesel fuels at full load conditions. It shows that higher CO emissions are observed at lower BP (near values of 25 kW to 35 kW) and start a sudden decrease with the increase in BP (36 kW to 46 kW). On the other hand, higher CO_2 emissions first decrease with increased BP (near values of 26 kW to 38 kW) and then start rising at BP above 39 kW. As predicted, higher CO emissions are noted for diesel fuel (hydrocarbon fuel) compared to biodiesel fuel (oxygenated fuel). Increased CO emissions from diesel fuel are observed due to partial combustion of hydrocarbons. When combustion happens in higher air–fuel mixtures with insufficient amounts of oxygen, it causes partial oxidation of hydrocarbons and leads to higher CO emissions. As depicted in Figs. 7 and 8, at more elevated BP, higher CO emissions are noticed for biodiesel blends compared to diesel. This is primarily attributed to the higher acid number of biodiesel fuels, as indicated in Table 3. Similar results are also observed by Agarwal et al. [74] and El-Zoheiry et al. [75], where increased CO emissions are noted for Jojoba biodiesel fuel due to its higher acid value exceeding the standard biodiesel limit. Compared to diesel, biodiesel has higher oxygen content in its chemical structures, influencing the combustion process and oxidising CO to CO_2 [76]. Hence, higher CO_2 emissions are observed with biodiesel blends compared to diesel fuel. Similar findings are also observed in studies by Coronado et al. [77], Thiyagarajan et al. [78] and Abed et al. [79].

The rate of oxidation depends on the temperatures inside the chamber. For instance, Fig. 8 depicts that the CO emissions are decreased with the increase in EGT. The high activation temperature oxides the hydrocarbon and release CO_2 emissions, as presented in Eq. (9).

$$CO + \frac{1}{2}O_2 \rightarrow CO_2 + Heat \tag{9}$$

3.3. Combustion characteristics

3.3.1. In-cylinder pressure

Fig. 9 illustrates the cylinder pressure variation for the TB10, UB10, TB20 and UB20 against the crank angle at 2400 rpm and full load conditions. The fuel type, air–fuel ratio, and engine operating condition influence peak pressure. Two peaks of cylinder pressure have been observed for all the fuels. Maximum peak is observed for the UB10 with 66.77 bar followed by UB10, Diesel, UB20, UB20 and UB10 with values 66.73 bar, 66.34 bar, 66.01 bar and 65.66 bar, respectively. On the second peak, TB10 showed maximum pressure observed as 60.31 bar, followed by UB10, UB20, TB20 and diesel with pressure values of 59.59 bar, 59.55 bar, 59.36 bar and 56.53 bar, respectively. As mentioned earlier, biodiesel has a higher viscosity and degree of evaporation, which

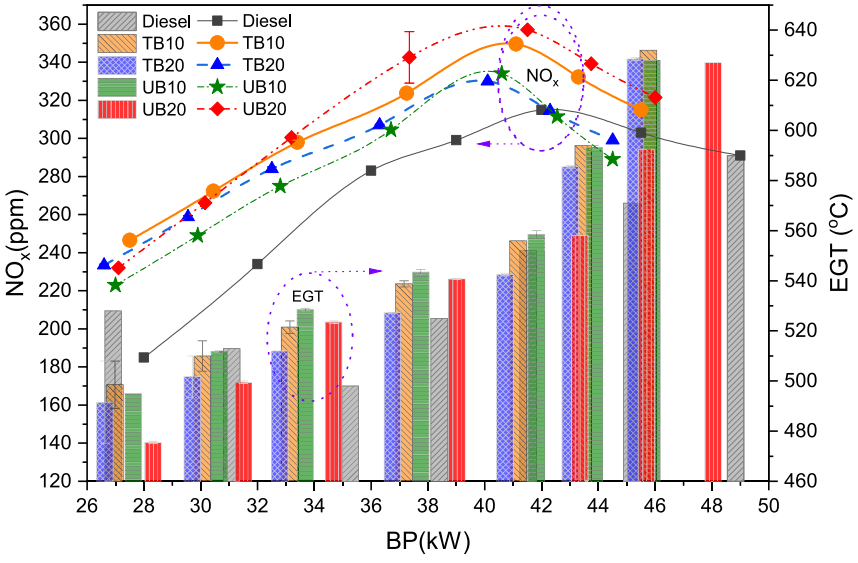

Fig. 6. Effect of Tucuma and Ungurahui oils on HC emissions with respect to BP.

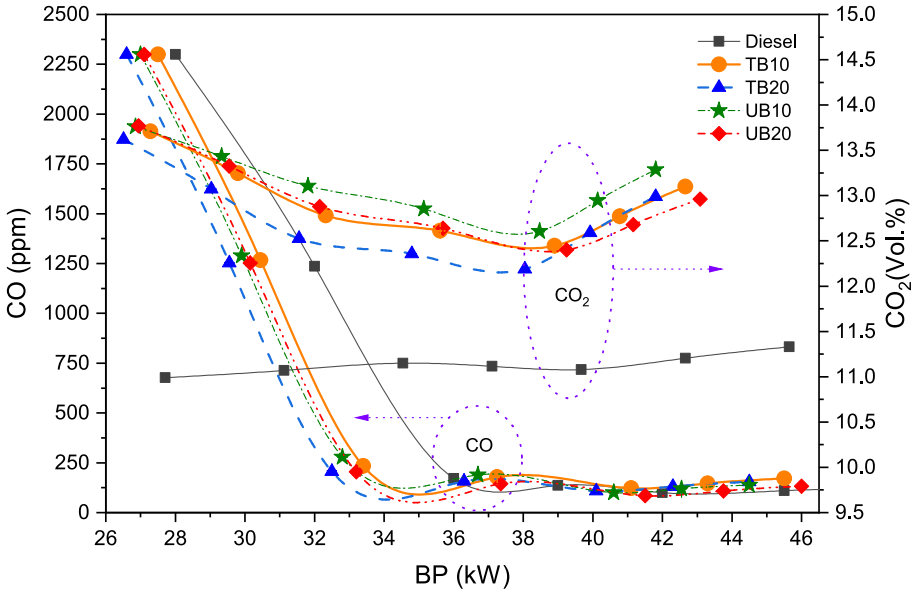

Fig. 7. Effect of variation in BP on CO and CO_2 emissions.

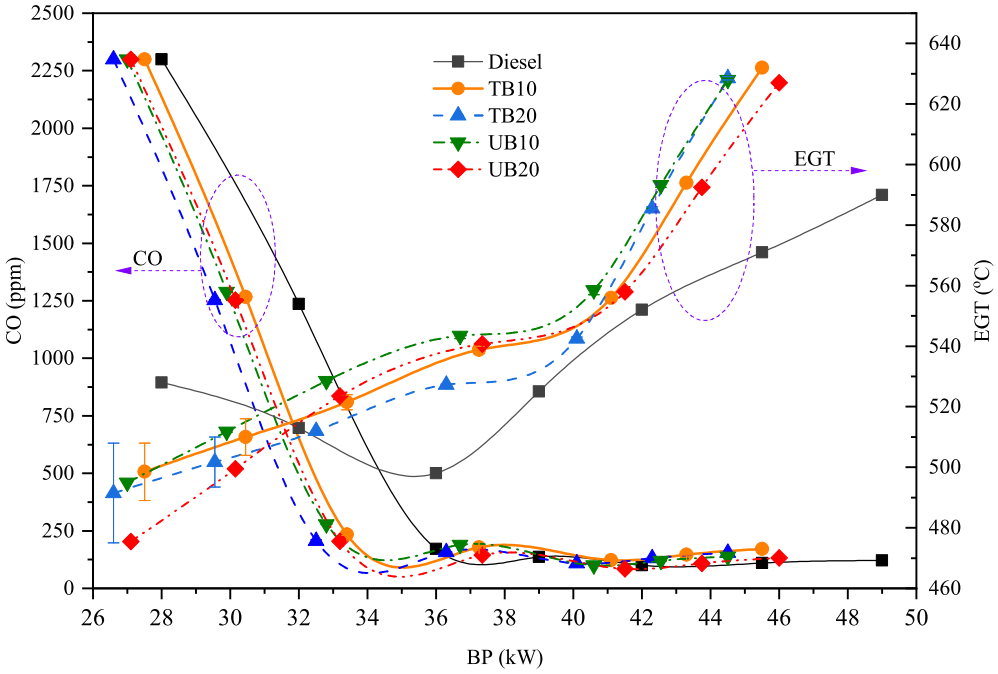

Fig. 8. Effect of BP and EGT on CO emission.

causes prolonged combustion [80]. As shown in Fig. 9, secondary peaks for the biodiesel blends are higher than the first due to the prolonged combustion. The higher viscosity and density of the fuels affect the droplet size, spray development and formation during combustion [81].

3.3.2. *Heat release rate (HRR)*

The net HRR for the Tucuma and Ungurahui biodiesel with respect to the crank angle is presented in Fig. 10. The study considered combustion analysis at full load conditions and at 2400 rpm to examine the peak heat release rates occurring at those conditions. Fig. 10 shows higher heat release rates for the TB10 and UB10 than for the diesel fuel. It is noted that a negative HRR trend is observed after the injection (352 °CA), where the combustible mixtures exhibit cooling effects as a result of fuel vapourization during the ignition delay period. TB10 has shown a higher peak of HRR at 371 °CA compared to all other fuel blends. In the case of TB10 and UB10, the marginal increase in BSFC has caused the peak HRR. The trend suggests that the HRR was decreased with the increase in biodiesel percentage in the blend. The lower calorific value of the biodiesel is one of the main reasons for the reduced HRR. Moreover, lower HRR for the UB20 and TB20 fuels are observed in the premixed combustion phase. Fuel density and viscosity have a significant effect during the premixed stage. Due to the higher density and viscosity of the biodiesel, the injected fuel droplets lose their kinetic energy on their way to better fuel atomization [82]. Though diesel has shown lower peak HRR during the premixed phase, higher HRR is noticed in the diffusion and late combustion phases. Lower viscous fuels increase fuel atomization and lead to a higher fuel evaporation rate, which increases the in-cylinder pressure and temperatures [83].

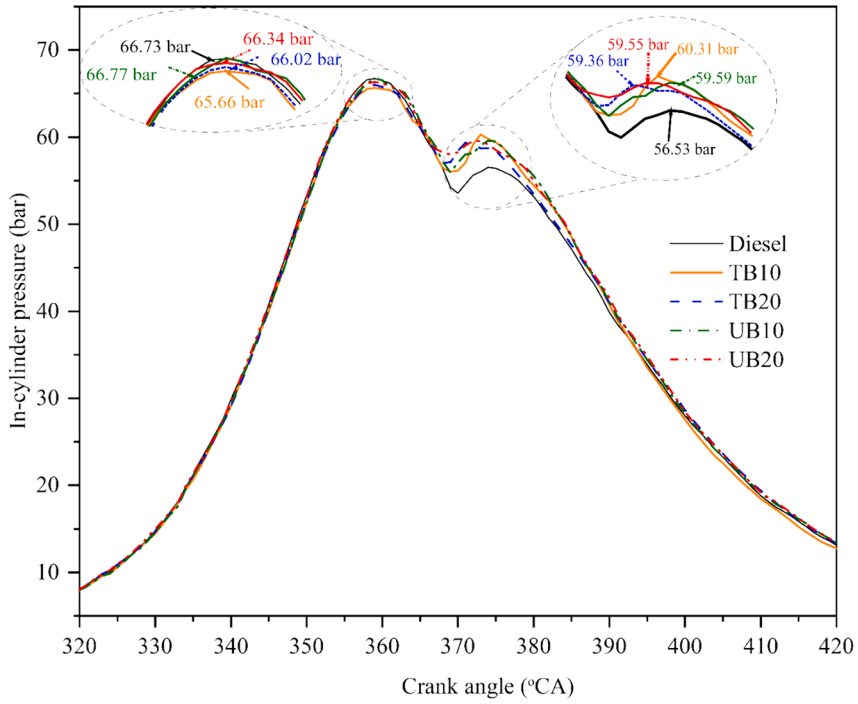

Fig. 9. In-cylinder pressure data for different biodiesel fuels at 2400 rpm and full load.

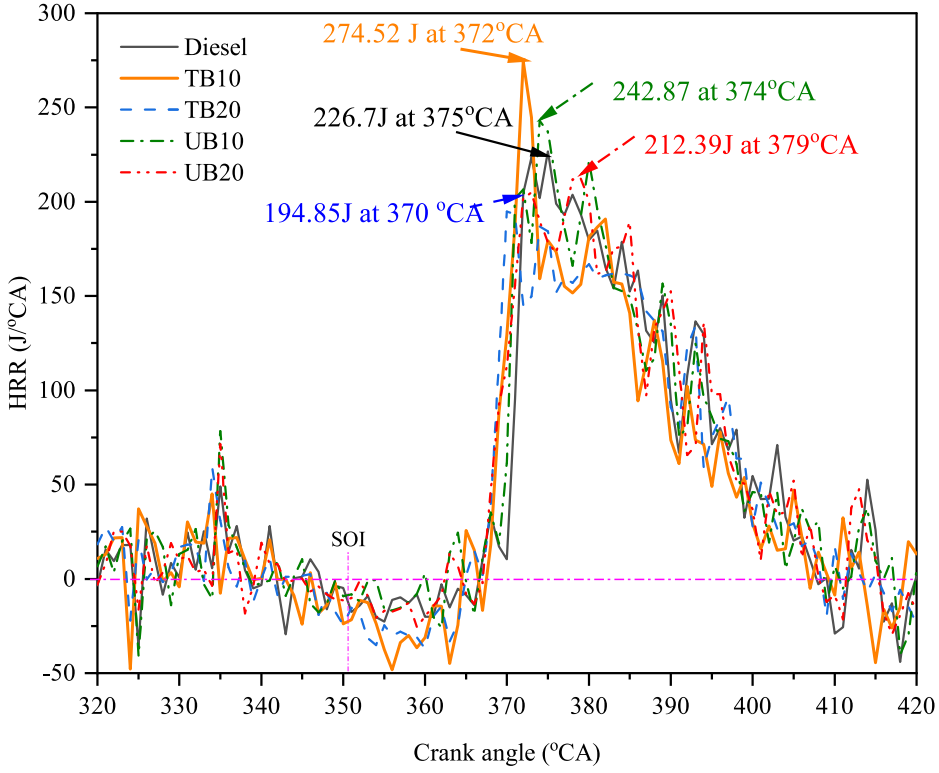

Fig. 10. Variation of heat release rate for Tucuma and biodiesel blends 2400 rpm and at full load.

For the cases of TB10 and TB20, shorter premixed combustion is observed than diesel fuel because of the early start of combustion (SOC). So, due to early SOC, the premixed fuel accumulates near the ignition delay period, which rapidly gets combusted and leads to high HRR for TB10 and TB20 fuels. A higher cetane number of biodiesel also plays a significant role in achieving a shorter ignition delay period with a high HRR.

3.3.3. *Mass fraction burnt (MFB)*

Fig. 11 presents the MFB of the investigated fuels at full load conditions. As depicted in Fig. 11, diesel has higher mass fraction burnt rates than others at 25 %, 50 % and 75 % burnt conditions. The main

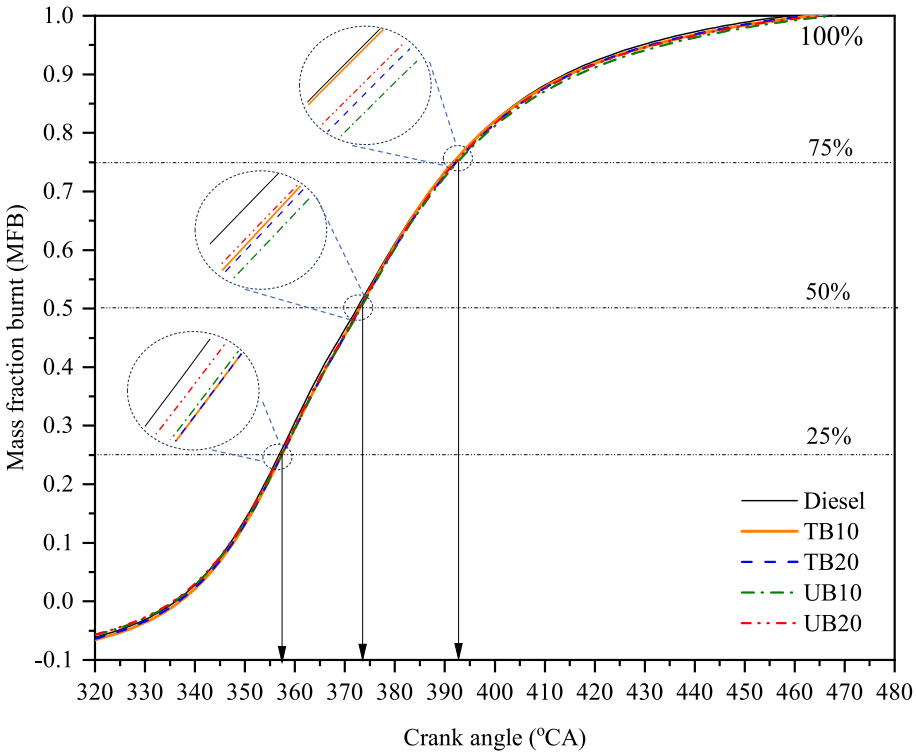

Fig. 11. Mass fraction burnt rates for Tcuma and biodiesel blends 2400 rpm and at full load.

reason is the larger spray droplets of biodiesel fuels compared to fossil diesel fuel. Fuel atomization time is longer for biodiesel fuels than diesel, which takes longer to get distributed into the chamber [84,85]. Similar results are also observed in the studies, where diesel exhibits a higher burnt rate than biodiesel fuel [86]. In the initial stages (25 %) and mid-stages (50 %), the burnt rate of UB20 showed a faster MFB than all other blends. During the 75 % mass fraction, the burnt rate is observed more for TB10, followed by UB20, TB20 and UB10. This is mainly due to biodiesel's higher boiling temperature range, which delays the SOC [86].

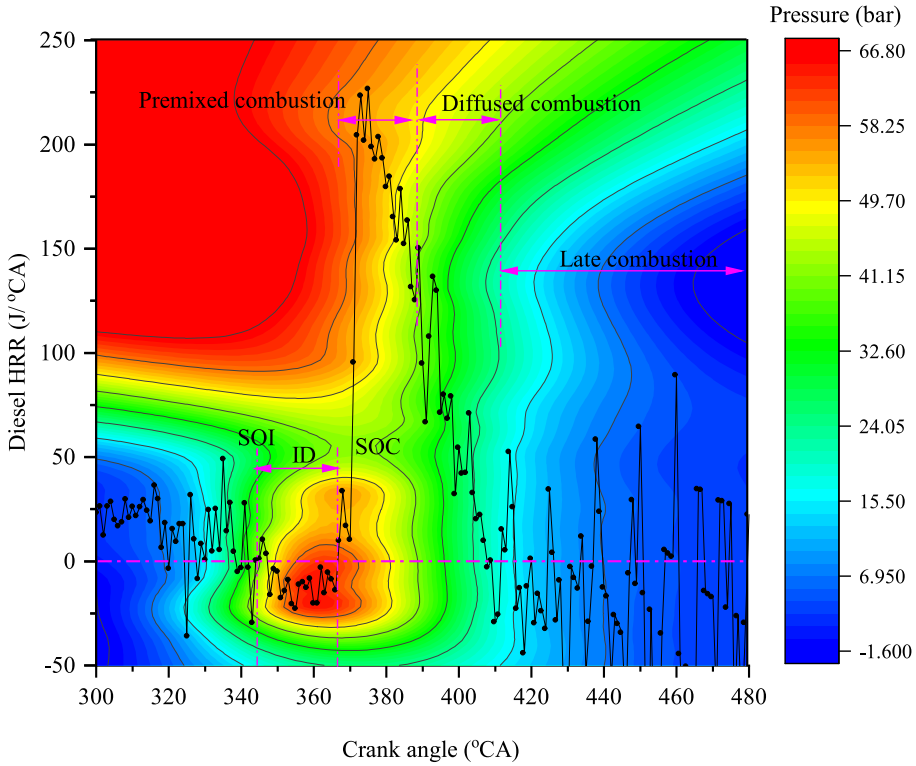

Fig. 12. Relationship between pressure and HRR for diesel fuel at 2400 rpm and full load condition.

3.3.4. Comparison of the relationship between pressure and HRR for different biodiesel blends

Figs. 12 to 16 illustrate the relationship between the pressure and heat release rate for the diesel, Tucuma and Ungurahui biodiesel blends. The SOC is early for biodiesel fuels compared to diesel fuel. SOC for diesel occurs early for UB20 at 366 °CA, followed by TB20, TB10, and UB10 and diesel at crank angles 367 °CA, 368 °CA, 369 °CA and 370 °CA, respectively. Even though no general conclusion can be drawn, it is observed that shorter ignition delay is observed for the higher biodiesel blends (TB20 and UB20) compared to UB10, TB10 and diesel fuel blends. Senatore et al. [87] observed from their investigation that ignition delay is shortened for soybean methyl ester compared to diesel. The authors attributed this to the lower viscosity of soybean methyl esters compared to diesel. In one study, Banapurmath et al. [45] revealed longer ID for honge, jatropha and sesame biodiesel fuels compared to diesel.

Peak pressures will greatly influence the HRR, which varies with blends. For all the blends in Figs. 12 to 16, the significant peak pressures (red regions from the contour graphs), can be observed near the combustion stage and during the injection period. The pressure distribution across the combustion stroke is different for all the fuels. It can be seen that high pressure is noticed more for the TB10 fuel during diffused and late combustion stages. Less peak pressure distributions are noticed with the higher biodiesel fuel blends, TB20 and UB20.

4. Conclusion and recommendations

The study conducted an experimental investigation of diesel engine performance, emissions and combustion characteristics using two prospective biodiesel blends. Four blends were prepared, tested, analyzed, and compared with diesel fuel. The following conclusions are drawn from this study.

1) The maximum BTE (35.45 %) is noted for diesel fuel, followed by TB10 (31.96 %), TB20 (31.34 %), UB10 (32.56 %), and UB20 (32.11 %). At lower BP, BSFC for TB10, TB20, UB10 and UB20 fuels increased by 11.2 %, 14.78 %, 11.623 % and 20.88 %, respectively, compared to diesel. Similarly, at higher BP, the BSFC is increased for TB10, TB20, UB10 and UB20 fuels by 11.27 %, 13.25 %, 27.84 % and 28.38 %, respectively, compared to diesel,
2) The blend TB10 has shown a lower HC emission than other blends. Compared to diesel, TB20, UB10, and UB20 have shown reduced HC at lower BP and slightly increased with the increase in BP. Similarly, higher CO emissions are noted for Tucuma and Ungurahui blends at higher BP. Moreover, higher NO_x emission is observed for the UB20, followed by TB10, UB10, TB20 and diesel fuel.
3) More peak pressure values are noted for the TB10 (60.31 bar), followed by UB10 (59.59 bar), UB20 (59.55 bar), TB20 (59.36 bar) and diesel (56.53 bar). Longer combustion phasing is noticed in all the blended fuels compared to diesel TB20, and UB20 has shown early SOC compared to TB10, UB10 and diesel, leading to shorter ID.
4) Compared with diesel, TB10 ensures better combustion and reduces HC and CO_2 with a slight increase in CO and NO_x emissions. Compared to other blends, TB20, UB10, and UB20, TB10 has shown better performance, lower BSFC, lower HC, high HRR, and a higher peak pressure rise. Overall, TB10 has demonstrated better results followed by diesel.

The study recommends further investigation on combustion strategies, such as chamber modifications and injection parameter alterations to reduce NO_x with TB10. In future, the research may focus on the feasibility of adding alcohols, esters, and nanoparticles to these blends to reduce harmful NO_x emissions. It is also recommended to consider the Tucuma blend for commercial application as the experimental conversion rate results showed higher yield and better performance similar to that of diesel.

CRediT authorship contribution statement

Arun Teja Doppalapudi: Writing – original draft, Visualization, Methodology, Investigation, Data curation, Conceptualization. **Abul Kalam Azad:** Writing – review & editing, Visualization, Supervision,

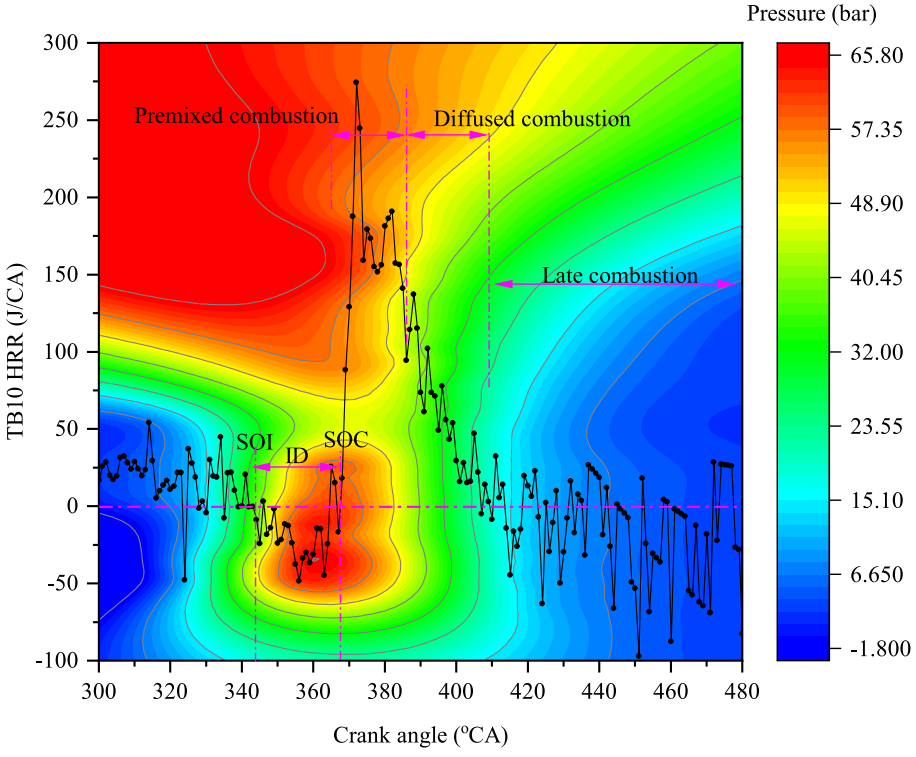

Fig. 13. Relationship between pressure and HRR for TB10 at 2400 rpm and full load condition.

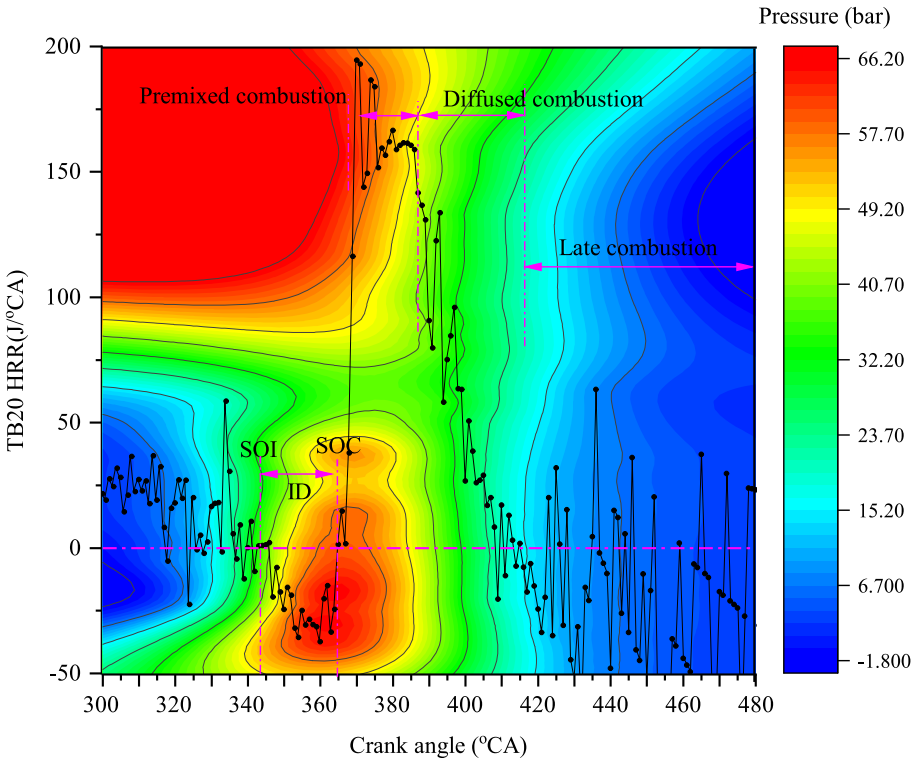

Fig. 14. Relationship between pressure and HRR for TB20 at 2400 rpm and full load condition.

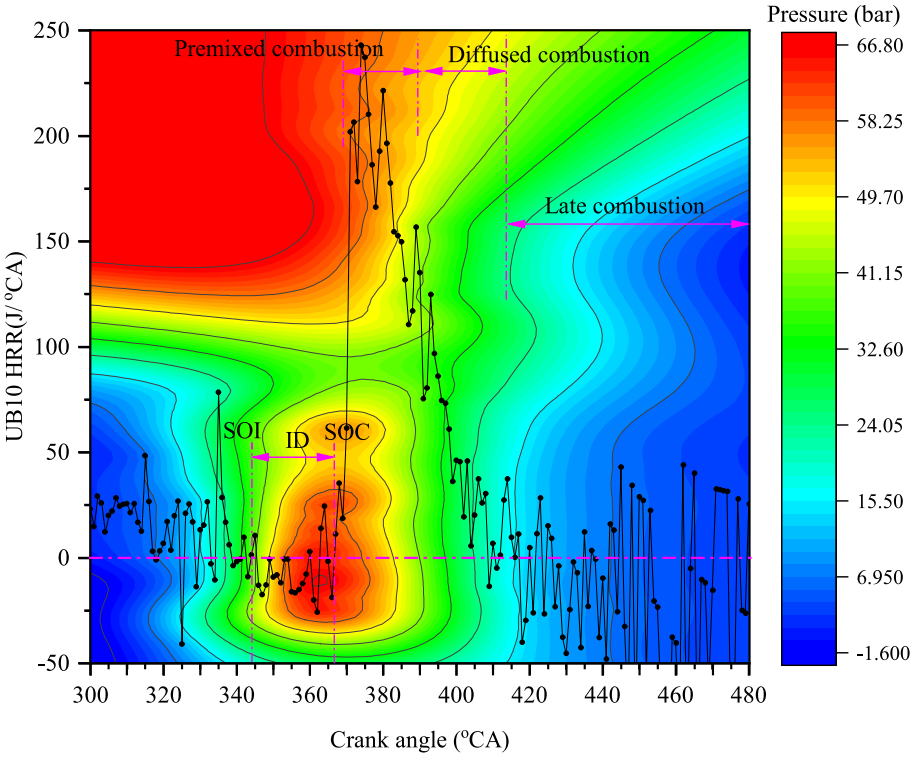

Fig. 15. Relationship between pressure and HRR for UB10 at 2400 rpm and full load condition.

Project administration, Conceptualization. **M.M.K. Khan:** Writing – review & editing, Supervision, Project administration.

Declaration of competing interest

The authors declare that they have no known competing financial interests or personal relationships that could have appeared to influence the work reported in this paper.

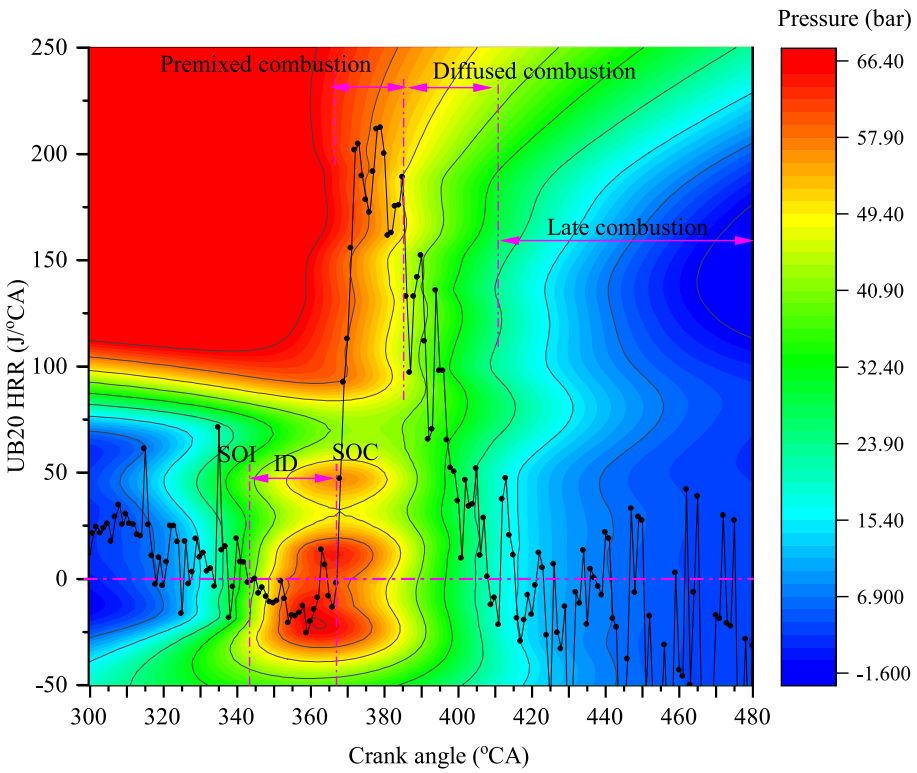

Fig. 16. Relationship between pressure and HRR for UB20 at 2400 rpm and full load condition.

Data availability

Data will be made available on request.

References

[1] Azad AK, Rasul MG, Khan MMK, Sharma SC, Hazrat MA. Prospect of biofuels as an alternative transport fuel in Australia. Renew Sustain Energy Rev 2015;43:331–51.

[2] Ashok B, Nanthagopal K, Saravanan B, Azad K, Patel D, Sudarshan B, et al. Study on isobutanol and Calophyllum inophyllum biodiesel as a partial replacement in CI engine applications. Fuel 2019;235:984–94.

[3] Halder P, Azad K, Shah S, Sarker E. 8 - Prospects and technological advancement of cellulosic bioethanol ecofuel production. In: Azad K, editor. Advances in Eco-Fuels for a Sustainable Environment. Woodhead Publishing; 2019. p. 211–36.

[4] Azad AK, Doppalapudi AT, Khan MMK, Hassan NMS, Gudimetla P. A landscape review on biodiesel combustion strategies to reduce emission. Energy Rep 2023;9:4413–36.

[5] Vasantha VL, Sharvari S, Alfia NS, Praveen N. Chapter 22 - Application of nanotechnology toward improved production of sustainable bioenergy. In: Kumar RP, Bharathiraja B, editors. Nanomaterials. Academic Press; 2021. p. 445–79.

[6] Vickram S, Manikandan S, Deena SR, Mundike J, Subbaiya R, Karmegam N, et al. Advanced biofuel production, policy and technological implementation of nano-additives for sustainable environmental management – a critical review. Bioresour Technol 2023;387:129660.

[7] IEA. *Renewables 2023, IEA, Paris*. 2024; Available from: https://www.iea.org/reports/renewables-2023.

[8] Statista. *Leading biodiesel producers worldwide in 2022*. 2024 [cited 2024 January 29]; Available from: https://www.statista.com/statistics/271472/biodiesel-production-in-selected-countries/.

[9] Sajjadi B, Raman AAA, Arandiyan H. A comprehensive review on properties of edible and non-edible vegetable oil-based biodiesel: composition, specifications and prediction models. Renew Sustain Energy Rev 2016;63:62–92.

[10] Azad AK, Jadeja AC, Doppalapudi AT, Hassan NM, Nabi MN, R.. Rauniyar *Design and Simulation of the Biodiesel Process Plant for Sustainable Fuel Production.* Sustainability 2024;16. https://doi.org/10.3390/su16083291.

[11] Bhuiya MMK, Rasul MG, Khan MMK, Ashwath N, Azad AK, Mofijur M. Optimisation of oil extraction process from australian native beauty leaf seed (Calophyllum Inophyllum). Energy Procedia 2015;75:56–61.

[12] Ong HC, Mahlia TMI, Masjuki HH, Norhasyima RS. Comparison of palm oil, Jatropha curcas and Calophyllum inophyllum for biodiesel: a review. Renew Sustain Energy Rev 2011;15(8):3501–15.

[13] Karmakar A, Karmakar S, Mukherjee S. Biodiesel production from neem towards feedstock diversification: Indian perspective. Renew Sustain Energy Rev 2012;16(1):1050–60.

[14] Nayak SK, Pattanaik BP. Experimental investigation on performance and emission characteristics of a diesel engine fuelled with mahua biodiesel using additive. Energy Procedia 2014;54:569–79.

[15] Ramadhas AS, Jayaraj S, Muraleedharan C. Biodiesel production from high FFA rubber seed oil. Fuel 2005;84(4):335–40.

[16] Hossain AK, Sharma V, Ahmad G, Awotwe T. Energy outputs and emissions of biodiesels as a function of coolant temperature and composition. Renew Energy 2023;215:119008.

[17] Information, N.C.f.B. *PubChem Compound Summary for CID 5364509, Methyl oleate*. 2024 [cited 2024 January 28]; Available from: https://pubchem.ncbi.nlm.nih.gov/compound/Methyl-oleate.

[18] Information, N.C.f.B. *PubChem Compound Summary for CID 8181, Methyl palmitate*. 2024 [cited 2024 January 28]; Available from: https://pubchem.ncbi.nlm.nih.gov/compound/Methyl-palmitate.

[19] Chen H, Ding M, Li Y, Xu H, Li Y, Wei Z. Feedstocks, environmental effects and development suggestions for biodiesel in China. J Traffic and Trans Eng (English Edition) 2020;7(6):791–807.

[20] Athar M, Zaidi S. A review of the feedstocks, catalysts, and intensification techniques for sustainable biodiesel production. J Environ Chem Eng 2020;8(6):104523.

[21] Dhar A, Agarwal AK. Experimental investigations of the effect of pilot injection on performance, emissions and combustion characteristics of Karanja biodiesel fuelled CRDI engine. Energ Conver Manage 2015;93:357–66.

[22] Gokalp B, Buyukkaya E, Soyhan HS. Performance and emissions of a diesel tractor engine fueled with marine diesel and soybean methyl ester. Biomass Bioenergy 2011;35(8):3575–83.

[23] Puhan S, Saravanan N, Nagarajan G, Vedaraman N. Effect of biodiesel unsaturated fatty acid on combustion characteristics of a DI compression ignition engine. Biomass Bioenergy 2010;34(8):1079–88.

[24] Sahoo P, Das L. Combustion analysis of Jatropha, Karanja and Polanga based biodiesel as fuel in a diesel engine. Fuel 2009;88(6):994–9.

[25] Singh D, Sharma D, Soni SL, Sharma S, Kumari D. Chemical compositions, properties, and standards for different generation biodiesels: a review. Fuel 2019;253:60–71.

[26] Raman LA, Deepanraj B, Rajakumar S, Sivasubramanian V. Experimental investigation on performance, combustion and emission analysis of a direct injection diesel engine fuelled with rapeseed oil biodiesel. Fuel 2019;246:69–74.

[27] Giakoumis EG, Sarakatsanis CK. Estimation of biodiesel cetane number, density, kinematic viscosity and heating values from its fatty acid weight composition. Fuel 2018;222:574–85.

[28] Yuan M-H, Chen Y-H, Chen J-H, Luo Y-M. Dependence of cold filter plugging point on saturated fatty acid profile of biodiesel blends derived from different feedstocks. Fuel 2017;195:59–68.

[29] Panchal B, Chang T, Kang Y, Qin S, Zhao Q, Wang J, et al. Synthesis of polymer based catalyst: optimization and kinetics modeling of the transesterification of Pistacia chinensis oil with diethyl carbonate using acidic ionic liquids. Fuel 2020; 276:118121.

[30] Giakoumis EG. A statistical investigation of biodiesel physical and chemical properties, and their correlation with the degree of unsaturation. Renew Energy 2013;50:858–78.

[31] Shameer PM, Ramesh K. Experimental evaluation on performance, combustion behavior and influence of in-cylinder temperature on NOx emission in a D.I diesel engine using thermal imager for various alternate fuel blends. Energy 2017;118: 1334–44.

[32] Lapuerta M, Rodríguez-Fernández J, Agudelo JR. Diesel particulate emissions from used cooking oil biodiesel. Bioresour Technol 2008;99(4):731–40.

[33] Sahoo PK, Das L, Babu M, Naik S. Biodiesel development from high acid value polanga seed oil and performance evaluation in a CI engine. Fuel 2007;86(3): 448–54.

[34] Tziourtzioumis D, Demetriades L, Zogou O, Stamatelos A. Experimental investigation of the effect of a B70 biodiesel blend on a common-rail passenger car diesel engine. Proce Institution of Mechanical Engineers, Part D: J Automobile Eng 2009;223(5):685–701.

[35] Mueller CJ, Boehman AL, Martin GC. An experimental investigation of the origin of increased NOx emissions when fueling a heavy-duty compression-ignition engine with soy biodiesel. SAE Int J Fuels Lubr 2009;2(1):789–816.

[36] Habibullah M, Masjuki HH, Kalam MA, Fattah IR, Ashraful A, Mobarak H. Biodiesel production and performance evaluation of coconut, palm and their combined blend with diesel in a single-cylinder diesel engine. Energ Conver Manage 2014;87: 250–7.

[37] Hazrat M, Rasul MG, Mofijur M, Khan M, Djavanroodi F, Azad A, et al. A mini review on the cold flow properties of biodiesel and its blends. Front Energy Res 2020;8:598651.

[38] Mota MFS, Ferreira MJA, Novaes FJM, Marriott PJ, Rezende CM, Freitas SP. Natural crystallisation of tucuma (Astrocaryum vulgare Mart.) pulp olein. J Food Compos Anal 2022;114:104795.

[39] Bora, P., N. Narain, R. Rocha, A. De Oliveira Monteiro, R. De Azevedo Moreira. (2001) *Characterisation of the oil and protein fractions of tucuma (Astrocaryum Vulgare Mart.) fruit pulp and seed kernel.* Ciencia y Tecnología Alimentaria. **3**(29): p. 111-116.

[40] Rodriguez-Amaya, D.B., *A guide to carotenoid analysis in foods*. Vol. 71. 2001: ILSI press Washington.

[41] Mushtaq M, Akram S, Hasany SM. Seje (Oenocarpus/Jessenia bataua) Palm Oil. In: Ramadan MF, editor. Fruit Oils: Chemistry and Functionality. Cham: Springer International Publishing; 2019. p. 883–98.

[42] Akram S, Sultana B, Asi MR, Mushtaq M. Salting-out-assisted liquid–liquid extraction and reverse-phase high-performance liquid chromatographic monitoring of thiacloprid in fruits and vegetables. Sep Sci Technol 2018;53(10): 1563–71.

[43] Mukhtar B, Mushtaq M, Akram S, Adnan A. Maceration mediated liquid–liquid extraction of conjugated phenolics from spent black tea leaves extraction of non-extractable phenolics. Anal Methods 2018;10(35):4310–9.

[44] wan nik ws, Maleque M, Ani F, Masjuki HH. Experimental investigation on system performance using palm oil as hydraulic fluid. Industrial Lubrication and Tribology 2007;59:200–8.

[45] Knothe G, Dunn RO. A comprehensive evaluation of the melting points of fatty acids and esters determined by differential scanning calorimetry. J Am Oil Chem Soc 2009;86(9):843–56.

[46] Knothe G, Razon LF. Biodiesel fuels. Prog Energy Combust Sci 2017;58:36–59.

[47] Doppalapudi AT, Azad AK. Advanced numerical analysis of in-cylinder combustion and NOx formation using different chamber geometries. Fire 2024;7. https://doi.org/10.3390/fire7020035.

[48] Doppalapudi AT, Azad AK, Khan MM. Analysis of improved in-cylinder combustion characteristics with chamber modifications of the diesel engine. Energies 2023;16. https://doi.org/10.3390/en16062586.

[49] Odibi C, Babaie M, Zare A, Nabi MN, Bodisco TA, Brown RJ. Exergy analysis of a diesel engine with waste cooking biodiesel and triacetin. Energ Conver Manage 2019;198:111912.

[50] Nabi MN, Rasul MG, Anwar M, Mullins BJ. Energy, exergy, performance, emission and combustion characteristics of diesel engine using new series of non-edible biodiesels. Renew Energy 2019;140:647–57.

[51] How H, Masjuki H, Kalam M, Teoh Y. An investigation of the engine performance, emissions and combustion characteristics of coconut biodiesel in a high-pressure common-rail diesel engine. Energy 2014;69:749–59.

[52] Azad AK, Halder P, Wu Q, Rasul MG, Hassan NMS, Karthickeyan V. Experimental investigation of ternary biodiesel blends combustion in a diesel engine to reduce emissions. Energy Conversion and Management: X 2023;20:100499.

[53] Mendera KZ, Spyra A, Smereka M. Mass fraction burned analysis. Journal of KONES Internal Combustion Engines 2002;3(4):193–201.

[54] Yin P, Prabhu L, Saranya SN, Devanesan S, Alsahi MS, Anderson A, et al. Effects of Scenedesmus dimorphus, spirulina biodiesel, hydrogen and nanoparticles fuel blends on mass burn fraction, emission, noise and vibration characteristics. Fuel 2023;352:129010.

[55] Tan YH, Abdullah MO, Nolasco-Hipolito C, Zauzi NSA, Abdullah GW. Engine performance and emissions characteristics of a diesel engine fueled with diesel-biodiesel-bioethanol emulsions. Energ Conver Manage 2017;132:54–64.

[56] Boehman AL, Morris D, Szybist J, Esen E. The impact of the bulk modulus of diesel fuels on fuel injection timing. Energy Fuel 2004;18(6):1877–82.

[57] Doppalapudi AT, Azad AK, Khan MMK. Advanced strategies to reduce harmful nitrogen-oxide emissions from biodiesel fueled engine. Renew Sustain Energy Rev 2023;174:113123.

[58] Gautam A, Agarwal AK. Experimental investigations of comparative performance, emission and combustion characteristics of a cottonseed biodiesel-fueled four-stroke locomotive diesel engine. Int J Engine Res 2012;14(4):354–72.

[59] Gad MS, El-Shafay AS, Abu Hashish HM. Assessment of diesel engine performance, emissions and combustion characteristics burning biodiesel blends from jatropha seeds. Process Saf Environ Prot 2021;147:518–26.

[60] Ağbulut Ü, Sarıdemir S, Albayrak S. Experimental investigation of combustion, performance and emission characteristics of a diesel engine fuelled with diesel–biodiesel–alcohol blends. J Braz Soc Mech Sci Eng 2019;41(9):389.

[61] Jaliliantabar F, Ghobadian B, Carlucci AP, Najafi G, Ficarella A, Strafella L, et al. Comparative evaluation of physical and chemical properties, emission and combustion characteristics of brassica, cardoon and coffee based biodiesels as fuel in a compression-ignition engine. Fuel 2018;222:156–74.

[62] Emma AF, Alangar S, Yadav AK. Extraction and characterization of coffee husk biodiesel and investigation of its effect on performance, combustion, and emission characteristics in a diesel engine. Energy Conversion and Management: X 2022;14: 100214.

[63] Venu H, Raju VD, Lingesan S, Elahi M Soudagar M. Influence of Al2O3nano additives in ternary fuel (diesel-biodiesel-ethanol) blends operated in a single cylinder diesel engine: performance, combustion and emission characteristics. Energy 2021;215:119091.

[64] Shareef SM, Mohanty DK. Experimental investigations of dairy scum biodiesel in a diesel engine with variable injection timing for performance, emission and combustion. Fuel 2020;280:118647.

[65] Elkelawy M, Alm-Eldin Bastawissi H, El Shenawy EA, Taha M, Panchal H, Sadasivuni KK. Study of performance, combustion, and emissions parameters of DI-diesel engine fueled with algae biodiesel/diesel/n-pentane blends. Energy Conversion and Management: X. 2021;10:100058.

[66] Paneerselvam P, Panithasan MS, Venkatesan G, Malairajan M. Optimization of common rail direct injection diesel engine performance with Melia dubia methyl ester peppermint oil blend using response surface methodology approach and investigation of hydrogen and hydroxy influence. Int J Hydrogen Energy 2024;50: 796–819.

[67] Doppalapudi AT, Azad AK, Khan MMK. Combustion chamber modifications to improve diesel engine performance and reduce emissions: a review. Renew Sustain Energy Rev 2021;152:111683.

[68] Chen H, Wang X, Pan Z. A comprehensive study of fuel composition, combustion and soot nanostructure characteristics of a diesel/light hydrocarbons premixed charge compression ignition engine. Fuel 2020;274:117858.

[69] Chen Z, Wang L, Zeng K. A comparative study on the combustion and emissions of dual-fuel engine fueled with natural gas/methanol, natural gas/ethanol, and natural gas/n-butanol. Energ Conver Manage 2019;192:11–9.

[70] Sanjid A, Masjuki HH, Kalam MA, Rahman SMA, Abedin MJ, Palash SM. Production of palm and jatropha based biodiesel and investigation of palm-jatropha combined blend properties, performance, exhaust emission and noise in an unmodified diesel engine. J Clean Prod 2014;65:295–303.

[71] Shi X, Yu Y, He H, Shuai S, Wang J, Li R. Emission characteristics using methyl soyate–ethanol–diesel fuel blends on a diesel engine. Fuel 2005;84(12):1543–9.

[72] Chou C-C, Huang P-C, Dai H-B. *An analysis of the performance characteristics of different cylinder temperatures for Ni-W and Ni-W-BN(h) plated piston rings in an air-cooled engine*. Energies 2022;15. https://doi.org/10.3390/en15031026.

[73] R, T. (2015) *Performance Analysis of Two Biodiesel Blended with Various Diesel Ratio.* International Journal of Innovative Research in Science, Engineering and Technology. **4**: p. 1816.

[74] Agarwal S, Kumari S, Mudgal A, Khan S. Green synthesized nanoadditives in jojoba biodiesel-diesel blends: an improvement of engine performance and emission. Renew Energy 2020;147:1836–44.

[75] El-Zoheiry RM, El-Seesy AI, Attia AMA, He Z, El-Batsh HM. Combustion and emission characteristics of Jojoba biodiesel-jet al mixtures applying a lean premixed pre-vaporized combustion techniques: an experimental investigation. Renew Energy 2020;162:2227–45.

[76] Babu D, Anand R. Chapter 14 - Biodiesel-diesel-alcohol blend as an alternative fuel for DICI diesel engine. In: Azad AK, Rasul M, editors. Advanced Biofuels. Woodhead Publishing; 2019. p. 337–67.

[77] Coronado CR, de Carvalho Jr JA, Silveira JL. Biodiesel CO2 emissions: a comparison with the main fuels in the Brazilian market. Fuel Process Technol 2009;90(2):204–11.

[78] Thiyagarajan S, Geo VE, Martin LJ, Nagalingam B. Comparative analysis of various methods to reduce CO2 emission in a biodiesel fueled CI engine. Fuel 2019;253: 146–58.

[79] Abed K, Gad M, El Morsi A, Sayed M, Elyazeed SA. Effect of biodiesel fuels on diesel engine emissions. Egypt J Pet 2019;28(2):183–8.

[80] Temizer İ, Cihan Ö, Eskici B. Numerical and experimental investigation of the effect of biodiesel/diesel fuel on combustion characteristics in CI engine. Fuel 2020;270:117523.

[81] IŞIk MZ. Comparative experimental investigation on the effects of heavy alcohols-safflower biodiesel blends on combustion, performance and emissions in a power generator diesel engine. Appl Therm Eng 2021;184:116142.

[82] Agarwal AK, Krishnamoorthi M, Singh H. Macroscopic and microscopic spray characterisation of Low-Octane blends for gasoline compression ignition engines. Fuel 2024;361:130346.

[83] Jing D, Zhang F, Li Y, Xu H, Shuai S. Experimental investigation on the macroscopic and microscopic spray characteristics of dieseline fuel. Fuel 2017;199:478–87.
[84] Karmakar B, Hossain A, Jha B, Sagar R, Halder G. Factorial optimization of biodiesel synthesis from castor-karanja oil blend with methanol-isopropanol mixture through acid/base doped Delonix regia heterogeneous catalysis. Fuel 2021;285:119197.
[85] Patel C, Agarwal AK, Tiwari N, Lee S, Lee CS, Park S. Combustion, noise, vibrations and spray characterization for Karanja biodiesel fuelled engine. Appl Therm Eng 2016;106:506–17.
[86] Fan M, Li Z, Song S, Alahmadi TA, Alharbi SA, Shanmugam S, et al. Optimizing biodiesel blends with green hydrogen fuel: a study on combustion duration, fuel mass burnt, engine performance and emissions. Fuel 2023;346:128340.
[87] Senatore, A., M. Cardone, V. Rocco, and M.V. Prati, *A comparative analysis of combustion process in DI diesel engine fueled with biodiesel and diesel fuel*. 2000: SAE International Warrendale, PA, USA.